An assessment of remote sensing-based drought index over different land cover types in southern Africa

Farai Maxwell Marumbwa[1,2,*], Moses Azong Cho[3,4] & Paxie W Chirwa [5]

[1]Centre for Environmental Studies, University of Pretoria, Pretoria, South Africa
[2]Research and Development Department, African Risk Capacity Sunhill Park, Johannesburg, South Africa
[3]Natural Resources and Environment Unit, The Council for Scientific and Industrial Research (CSIR), Pretoria, South Africa
[4]Department of Plant and Soil Science, University of Pretoria, Pretoria, South Africa
[5]Forest Science Postgraduate Programme, Department of Plant and Soil Sciences, University of Pretoria, Pretoria, South Africa

*Contact: Farai Maxwell Marumbwa. Email: iconmaxmarumbwa@gmail.com
Research and Development Department, African Risk Capacity Sunhill Park, Building 1, Sunhill Park, 1 Eglin Road, Sunninghill, Johannesburg, South Africa

ABSTRACT

An understanding of drought and land cover interaction plays a crucial role in vegetation vulnerability studies and land use planning. However, there is paucity of information on drought, land cover and land use interaction in southern Africa. We analysed the drought impact on land cover using Globcover land cover data and Vegetation Condition Index (VCI) for the 2015 to 2016 season. The 2015 to 2016 season was chosen because it was the worst drought in southern Africa since the 1980s. We developed a novel land cover 'social pixels' or 'village pixels' which represents rural communities. The Kruskal–Wallis test was used to evaluate whether there is a significant difference in drought impact among the land cover classes. The response of each land cover to drought impact was calculated by correlating Standardized Precipitation Evapotranspiration Index (SPEI) and Normalized Difference Vegetation Index (NDVI). Our results reveal that the evergreen forests and the flooded vegetation were the most severely affected by the 2015–2016 drought. However, the lowest VCI values were recorded within the village pixels land cover, indicating the vulnerability of rural communities to drought impacts. The vegetation response to drought impact ranged from 2 months (crops) to 8 months (flooded vegetation). With regards to drought recurrence (1998 to 2018), the crop and grassland land cover recorded the highest drought frequency whilst the forest had the least drought frequency.

KEYWORDS: Drought; Land cover; Land uses; Southern Africa; Vegetation; VCI

1. Introduction

Drought impact assessment on different land cover types is crucial for various agricultural and environmental applications (Baniya et al. 2019). Drought is a complex phenomenon and is regarded as one of the serious natural hazards with significant impacts on ecosystems (Wilhite 2000). Drought monitoring and assessment are complicated by the fact that there is no universal definition of drought. A number of definitions have been proposed with drought being regarded as diminished precipitation, soil moisture, plant vigour, ecological and socio-economic status (Kogan, Guo, and Yang 2019). In this study, we regard drought as a period when rainfall is below the historical mean (i.e. meteorological drought).

Various meteorological drought indices have been developed for drought monitoring based on data from meteorological stations (Vicente-Serrano, Beguería, and López-Moreno 2010) (e.g. Standardized Precipitation Evapotranspiration Index (SPEI)) Standardized Precipitation Index (SPI) and Palmer Drought Severity Index (PDSI) (Van Loon 2015). Of all these indices, the SPEI is the most commonly used. The SPEI is used to represent the anomalies of the water balance with negative SPEI values less than −1 indicative of meteorological drought (Vicente-Serrano 2007). SPEI algorithm makes use of both precipitation and an estimation of evapotranspiration (Vicente-Serrano, Beguería, and López-Moreno 2010) and it is available at multiple time-scales which makes it suitable for assessing the response of vegetation to meteorological drought impact (Vicente-Serrano 2007; Beguería et al. 2014).

The simultaneous analysis of meteorological drought impact on multiple land cover types at regional scale is crucial for quantifying the environmental impacts of droughts especially in the context of climate change (Vicente-Serrano 2007). This is more critical because drought impacts on vegetation can influence regional land cover type stability and transformation of the vegetation landscape (Tollerud et al. 2018).

Within the semi-arid regions, rainfall and temperature are the main drivers of drought (Nicholson, Davenport, and Malo 1990). Global climate models suggest a decrease in rainfall in southern Africa (Dai 2013). This projected decrease of rainfall will intensify drought occurrence and degradation of land (Vicente-Serrano 2007) thereby impacting crops and livestock (Ayanlade et al. 2018). As such it is critical to assess drought and land cover interaction. A number of studies have reported drought impact on single land cover types mostly focusing on crop, e.g. (Tollerud et al. 2018; Kuri et al. 2019; Gidey et al. 2018; Kogan 1995). There are very few studies that have focused on the analysis of drought impacts on land cover types which are dominated by rural communities ('social pixels' or 'village pixels').

The analysis of drought impact on land cover especially focusing on 'village pixel' is important considering that more than 57% of the southern African people live in rural areas (Dalal-clayton 1997). Most of these rural populations survive on the ecosystem services with little adaptive capacity to cope with weather impacts which makes them vulnerable to drought. The monitoring and assessment of drought impact at village pixel are therefore crucial. Up to now, no attempt has been made to understand drought impacts within the 'village pixels'. This is largely due to the absence of the land cover type which represents the social pixels or rural communities.

Traditional approaches for quantifying drought and land-use interactions are mainly based on point data from meteorological ground stations (Vicente-Serrano 2007). The problem of this approach is that it is limited in space and time and is mostly suited for localized applications (Rojas and Ahmed 2017). Furthermore, when using this approach, it is difficult to differentiate drought impacts among land cover types especially over large areas (Vicente-Serrano 2007). The use of remote sensing presents a potential solution as it provides both vegetation and rainfall indicators relevant for drought monitoring (Liu and Kogan 1996). The main advantage of remote sensing is that it provides a wide coverage and a large historical archive of data. This makes it ideal for regional assessments of drought impact on vegetation (Kogan 1995).

The Normalized Difference Vegetation Index (NDVI) is the most commonly used remote sensing index for monitoring the vegetation condition. NDVI is widely used to monitor vegetation status and is highly correlated to biomass (Tucker et al. 1983). However, due to the fact that NDVI is also influenced by relief, ecosystem characteristics, underlying geology, and phenology (Kogan 1990), NDVI on its own is not useful for comparing drought impact on vegetation across different land cover types (Vicente-Serrano 2007). In this regard, Kogan (1990) developed the Vegetation Condition Index (VCI) which applies a geographic filter to remove the influence of ecosystem and topography on NDVI and assess the drought impact on vegetation (Vicente-Serrano 2007; Jain et al. 2009). The resulting VCI has values ranging between 0 (minimum NDVI) and 100 (maximum NDVI). The low and high VCI values indicate drought or no drought condition on vegetation, respectively (Kogan 1995). VCI therefore provides a quick overview of how well the vegetation is growing and is widely used for monitoring the impact of weather (i.e. meteorological drought) on plants across diverse land cover types (Vicente-Serrano 2007). Research studies, e.g., (Kogan 1997; Dutta et al. 2015) and by the United Nations Platform for Space-based Information for Disaster Management and Emergency Response (UN-SPIDER) indicate that drought impact on vegetation is indicated by VCI values below 40 with VCI values less than 30 showing moderate to extreme drought conditions (UN-SPIDER 2019).

In this study, we tested if there is a significant difference in the mean drought impact on vegetation (VCI_{mean}) among the land cover types using the 2015 to 2016 season. The VCI_{mean} is defined as the average seasonal VCI computed from the dekadal VCI images. The 2015 to 2016 season was one of the most severe droughts in the history of southern Africa (Archer et al. 2017; Swemmer et al. 2018). In addition, the study also focused on answering the following questions: which land cover has the highest drought severity and frequency? How does the land cover types respond to drought impact? We analysed the response of each land cover to drought by correlating the vegetation data (NDVI) with SPEI.

2. Materials and methods

2.1. Study area

The study area is located in southern Africa and is bounded by the following coordinates: 6°N to 35°S and longitude 10°E to 41°E. The southern half of the region is mainly dominated by the Grassland (Figure 1). The forests land cover type is mainly located in the northern parts of the region. Vegetation development in the study area is mainly determined by precipitation availability. Most parts of the study area receive summer rainfall between October and April. The Cape Province of South African receives winter rainfall between May and September. The highest rainfall values are recorded in the northern parts of the region mainly covering the forest areas and the lowest rainfall is received in the south western parts of the study area mainly covering the grasslands.

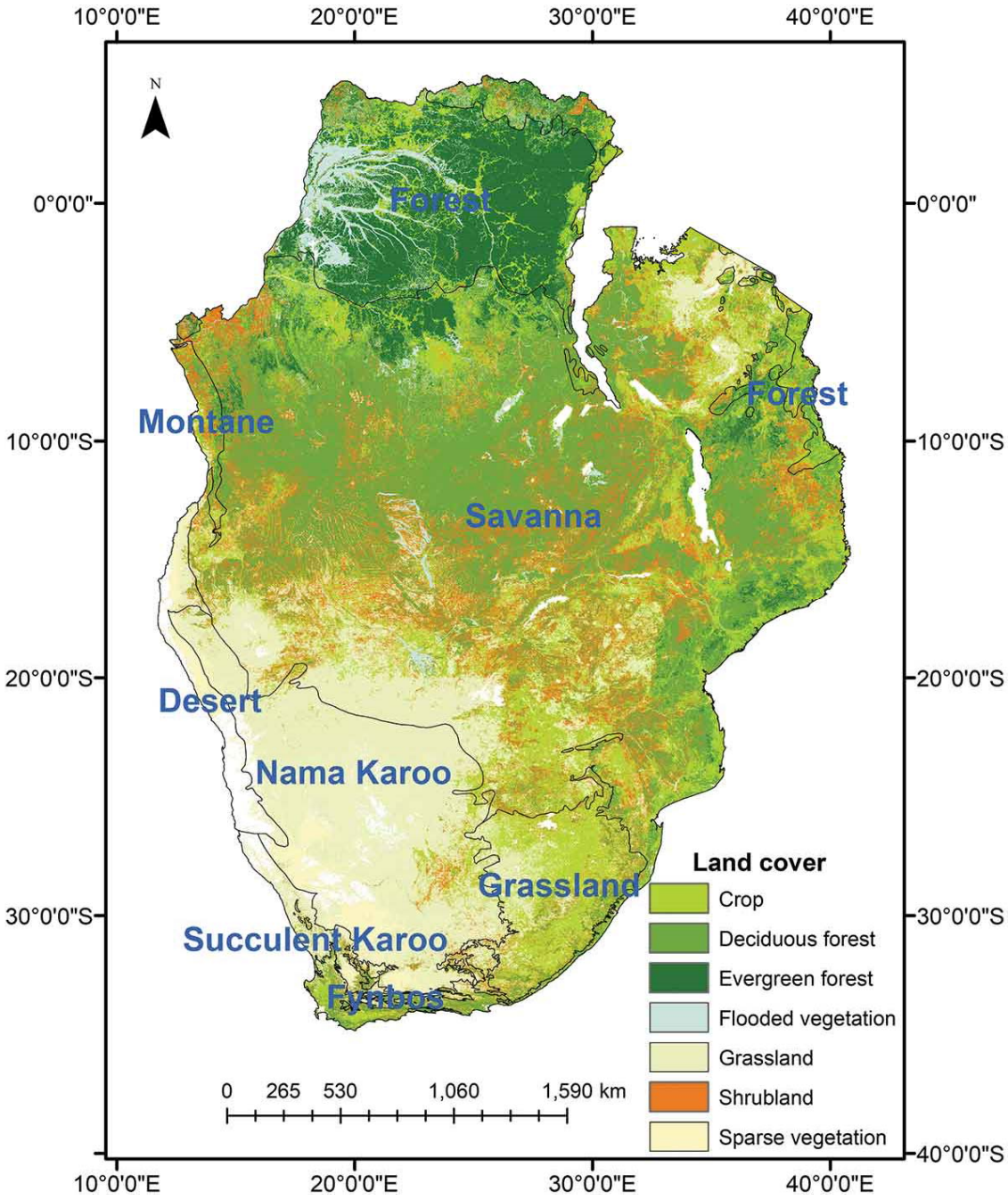

Figure 1. Location of the study area showing land cover distribution.

The rainfall variability is mainly controlled by the El Niño Southern Oscillation (ENSO) which is triggered by variations in the sea surface temperatures in the equatorial Pacific ocean (Unganai and Kogan 1998). The warm phase of the ENSO (El Niño) results in drought over most parts of southern Africa whilst the cold phase of the ENSO (La Niña) results in floods (Lindesay 1988). Some of the strongest El Niño events in southern Africa are 1982 to 1983 and 2015 to 2016 rainfall seasons which resulted in severe droughts (Davis-Reddy and Vincent 2017).

2.2. Data

2.2.1. NDVI

In this study, we used the NDVI data based on the Satellite Pour l'Observation de la Terre (SPOT-VGT) and Project for On-Board Autonomy – Vegetation (PROBA-V) sensor. This data is produced every 10 days using the Maximum Value Composite (MVC) technique to reduce the impacts of cloud cover (Wolters et al. 2016). The data is produced at a spatial resolution of 1 km from 1998 to present and is available from Copernicus website (https://land.copernicus.eu/global/products/ndvi). NDVI provides information about vegetation greenness and is computed using Equation (1).

$$\mathrm{NDVI} = \frac{(\mathrm{NIR}) - R_{\mathrm{Red}}}{(\mathrm{NIR}) + R_{\mathrm{Red}}} \quad (1)$$

Where NIR is the near-infrared reflectance and R_{Red} is the visible red reflectance (Vicente-Serrano 2007). To minimize the effects of cloud contamination inherent in NDVI data, we applied a Savitzky–Golay smoothing filter (5 window filter, 5^{th} order polynomial) following (Cho, Ramoelo, and Dziba 2017). The resultant smoothed NDVI was used to calculate VCI.

2.2.2. VCI

For the purposes of comparing the drought impact among the land cover types and performing drought impact frequency analysis, we used the NDVI to compute the VCI at 10 days (dekad) and seasonal intervals using Equation (2) (Kogan 1990).

$$\mathrm{VCI} = \frac{(\mathrm{NDVI}) - (\mathrm{NDVI}_{\mathrm{min}})}{(\mathrm{NDVI}_{\mathrm{max}}) - (\mathrm{NDVI}_{\mathrm{min}})} \times 100 \quad (2)$$

Where NDVI is the 10 day or seasonal vegetation index, NDVI_{max} NDVI_{min} is the long-term maximum and minimum calculated for each pixel for each dekad or season from the NDVI time-series data. The resulting VCI values range from 0 (extreme drought) and 100 (no drought) (Kogan 1995). Drought impact on vegetation is indicated by VCI values below 40 with VCI values less than 30 showing moderate to extreme drought conditions (UN-SPIDER 2019).

2.2.3. SPEI

We used SPEI to assess the response of each land cover type to drought impact by correlating it with NDVI. SPEI data were downloaded from the following website: https://digital.csic.es/handle/10261/153475. The SPEI data are provided at multiple time-scales (1–48 months) at a spatial resolution of 0.5° (Vicente-Serrano, Beguería, and López-Moreno 2010).

2.3. Land use & land cover data

To analyse the impact of drought on each of land cover type we used the Globcover 2009 land cover data which is available on Google Earth (GGE) (Image ID: ESA/GLOBCOVER_L4_200901_200912_V2_3). The Globcover 2009 was developed by the European Space Agency (ESA) based on the Environmental Satellite (ENVISAT's) Medium Resolution Imaging Spectrometer (MERIS) Level 1B data (ESA 2019). The land cover data are provided at a spatial resolution of 300 m resolution with 23 land cover classes (Table 1). To simplify the analysis of drought impact on land cover classes, the original 23 land cover classes were reclassified to 11 classes as shown in (Table 2). These new classes were then used for assessing and comparing the drought impact on vegetation across the land cover types.

Table 1. Original globcover land cover classes.

Value	Label
11	Post-flooding or irrigated croplands (or aquatic)
14	Rainfed croplands
20	Mosaic cropland (50 to70%)/vegetation (grassland/shrubland/forest) (20 to 50%)
30	Mosaic vegetation (grassland/shrubland/forest) (50 to 70%)/cropland (20 to 50%)
40	Closed to open (>15%) broadleaved evergreen or semi-deciduous forest (>5 m)
50	Closed (>40%) broadleaved deciduous forest (>5 m)
60	Open (15–40%) broadleaved deciduous forest/woodland (>5 m)
70	Closed (>40%) needle leaved evergreen forest (>5 m)
90	Open (15–40%) needleleaved deciduous or evergreen forest (>5 m)
100	Closed to open (>15%) mixed broadleaved and needle leaved forest (>5 m)
110	Mosaic forest or shrubland (50 to 70%)/grassland (20 to 50%)
120	Mosaic grassland (50 to 70%)/forest or shrubland (20 to 50%)
130	Closed to open (>15%) (broadleaved or needleleaved, evergreen or deciduous) shrubland (<5m)
140	Closed to open (>15%) herbaceous vegetation (grassland, savannas or lichens/mosses)
150	Sparse (<15%) vegetation
160	Closed to open (>15%) broadleaved forest regularly flooded (semi-permanently or temporarily) - Fresh or brackish water
170	Closed (>40%) broadleaved forest or shrubland permanently flooded - Saline or brackish water
180	Closed to open (>15%) grassland or woody vegetation on regularly flooded or waterlogged soil - Fresh, brackish or saline water
190	Artificial surfaces and associated areas (Urban areas >50%)
200	Bare areas
210	Water bodies
220	Permanent snow and ice
230	No data (burnt areas, clouds,)

Table 2. Reclassified globcover land cover classes.

Original class	New class	Name
11	1	Irrigated cropland
14, 20, 30	2	Crops
40,70, 90	3	Evergreen forest
50,60,100	4	Deciduous forest
110,120,130	5	Shrubland
140	6	Grassland
150	7	Sparse vegetation
160,170,180	8	Flooded vegetation
190, 200	9	Bare and artificial areas
210	10	Water bodies
220, 230	11	Ice and no data

The land cover data were also used to mask out built-up areas, waterbodies, bare soil, and irrigated crops from the analysis. The basic pre-processing of the Globcover data (i.e.

clipping global land cover data to the study area) was done using the google earth engine platform.

2.4. Livestock density data

We used the livestock (cattle and goats) density gridded data to compute the 'social pixels' or 'village pixels', a unique and novel land cover type representing rural communities. The livestock density map was used in developing the 'village pixel' land cover map because of the close association between rural communities with livestock especially cattle which is used as draught power (Ellis-Jones and O'Neill 2000; Pearson and Vall 1998). In addition, the village pixels also provide the rural communities with the ecosystem goods and service which support livelihoods (Cousins 1999). The village pixel land cover help to understand drought impacts on rural village communities and this helps in identification of rural communities which are vulnerable to drought impacts.

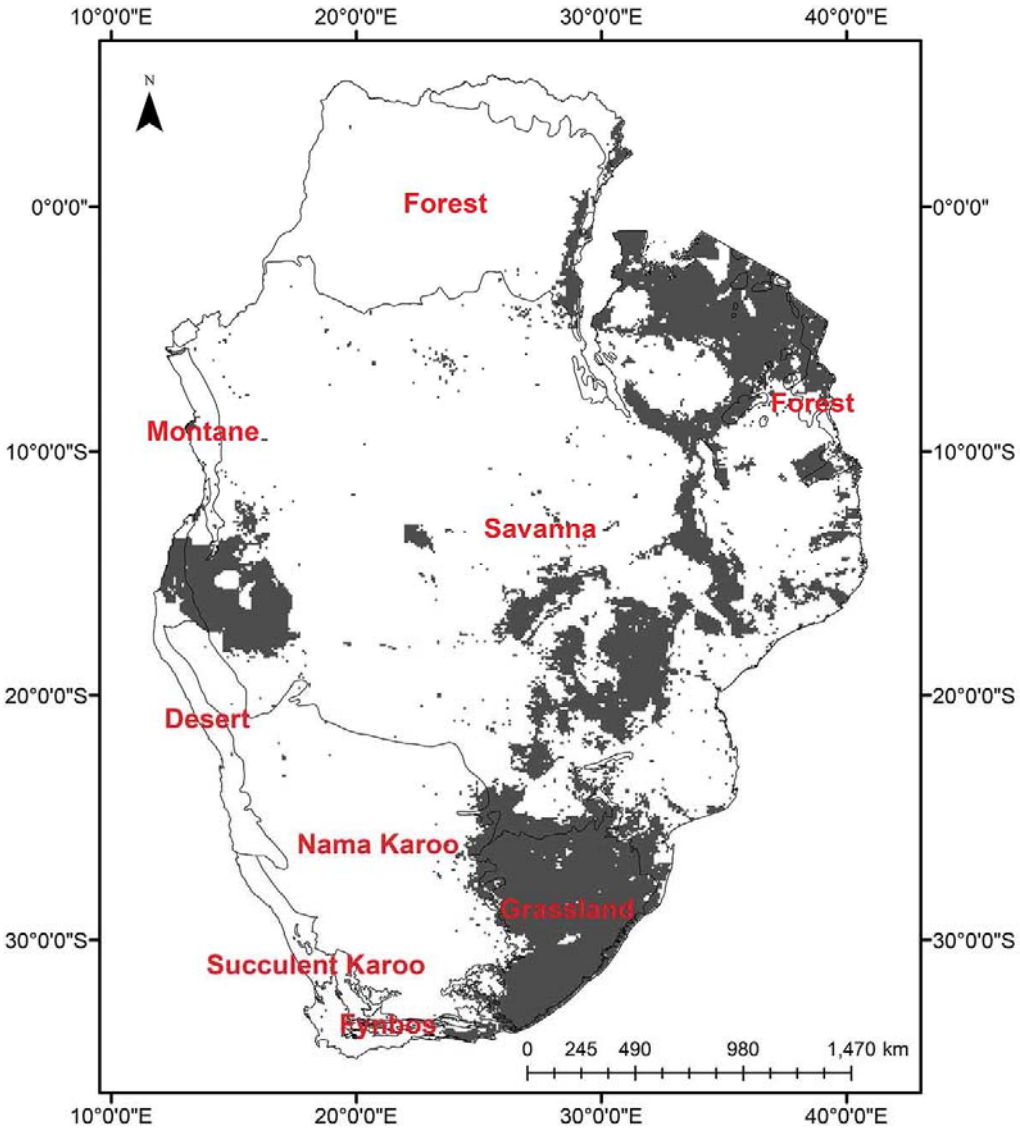

Figure 2. Village pixel map based on livestock density data.

The livestock gridded density data were downloaded from the Food and Agriculture Organization (FAO) geoportal: http://www.fao.org/geonetwork/srv/en/. This data is provided on a spatial resolution of 10 km and the data is adjusted to the Food and Agriculture Organization Corporate Statistical Database (FAOSTAT) values (Robinson et al. 2014). The 'village pixels' were defined as areas with cattle or goat density >900 per 10 km. The resultant village pixel land cover map (Figure 2) corresponds very well with the general rural population distribution patterns of southern Africa which makes it useful for understanding drought impacts on rural communities. This new land cover map was then used in the analysis together with other land cover types from the Globcover map.

2.5. Data analysis

In this study, we used two drought indices (i.e. VCI and SPEI) separately for two purposes. Firstly, the SPEI which is used for representing anomalies of the water balance (i.e. meteorological drought) was used for assessing the response of vegetation to water deficit by correlating SPEI (drought) with NDVI (vegetation). Secondly, the VCI was used for assessing the drought impact across the land cover types (i.e. assessing drought impacts on vegetation).

2.6. Assessment of drought impact among the land cover types

To assess drought impact across land cover types, we used a thresholding approach on the dekadal (10 days) VCI for 2015 to 2016 season. In order to identify the vegetation impacted by drought, we masked out pixels with VCI greater than 40 following UN-SPIDER (2019). A total of 21 dekadal VCI images were used in the analysis. We chose the 2015 to 2016 season because it was one of the driest since the 1980s, with severe consequences on vegetation (Archer et al. 2017). To test if there is any significant difference in drought impact among the land cover types, we first extracted the median VCI for each land cover type and then used the Kruskal–Wallis test (Kruskal and Wallis 1952) to determine whether there is a significant difference (p-value < 0.05) in the median VCI (drought impact) among the land cover types following recommendation by (Vargha and Delaney 1998). The Kruskal–Wallis test extends from the Wilcoxon Rank-Sum test which is used for two samples (Zaiontz 2019) and was used in place of one-way Analysis of Variance (ANOVA) since the VCI data were not normally distributed.

2.7. Land cover response to drought impact

To determine the response of the different land cover types to drought impact, we correlated the monthly NDVI data for 2015 to 2016 season with monthly SPEI data at different time-scales (i.e. 1,3,6,9,12, 18 and 24 months). We used NDVI for the correlation because it is an intuitive indicator of vegetation greenness and has been widely used in similar studies e.g. (Gouveia et al. 2017; Vicente-Serrano 2007; Vicente-Serrano, Beguería, and López-Moreno 2010; Vicente-Serrano et al. 2013). To facilitate the correlation, we first resampled the SPEI to match the 1 km resolution of the NDVI. We then computed a pixel-wise Mann-Kendal tau correlation coefficient (p-value < 0.05) between the monthly SPEI and NDVI for all the pixels. From the resultant correlation maps, we created a raster stack using R software (R Core Team 2018) and extracted the maximum correlation coefficient for each

pixel. Based on the resultant map of maximum correlation coefficient, we computed a map showing the SPEI time-scale at which maximum correlation is found. The SPEI time-scale with the maximum correlation is also referred to as the time lag of vegetation response to drought impact (Gouveia et al. 2017; Vicente-Serrano 2007; Vicente-Serrano, Beguería, and López-Moreno 2010; Vicente-Serrano et al. 2013). Results of the analysis were then summarized per each land cover.

2.8. Calculation of drought frequency

We calculated the seasonal drought frequency using the VCI_{mean} (seasonal VCI average) (October to April) data from 1998 to 2018. To calculate the drought frequency, we first created a boolean map from the seasonal VCI images which shows pixels affected by drought based on a thresholding of the seasonal VCI (i.e. VCI< 40) based on UN-SPIDER (2019) VCI classification. From the resultant boolean map, we then counted the number of times (i.e. years) each pixel was affected by drought condition (i.e. VCI<40) between the period 1998 to 2018. The results of the analysis were saved as a map to facilitate easy visual interpretation.

3. Results

3.1. Comparison of drought impact among the land cover classes

Results of the comparison of drought impact on vegetation for the different land cover types are shown in Figure 3. Each dot on the land cover type represents a dekad (10-day period) during the 2015 to 2016 vegetation-growing season. The village pixel land cover type recorded the lowest VCI (more drought impact) during the 2015 to 2016 season. This was followed by the flooded vegetation. The highest VCI_{mean} values were recorded in the grassland and the Sparse vegetation land cover types.

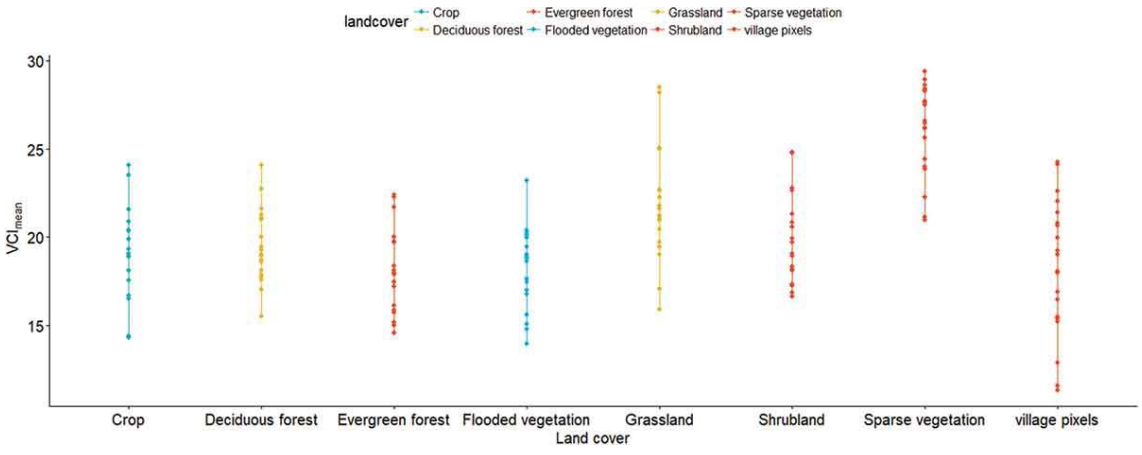

Figure 3. Drought impact for each land cover type based on dekadal VCI.

The box plots (Figure 4) provide a comparison of the drought impacts for the eight land cover types. The Kruskal–Wallis test shows that there is a significant difference in drought impact among the land cover types (p-value = $4.256e^{-11}$) confirming the fact that drought impact on vegetation is not the same across the land cover types. The low VCI values across

all the land cover which is indicative of extreme drought conditions were also reported by Archer et al. (2017) who did a similar study over southern Africa focusing on the 2014 to 2016 seasons.

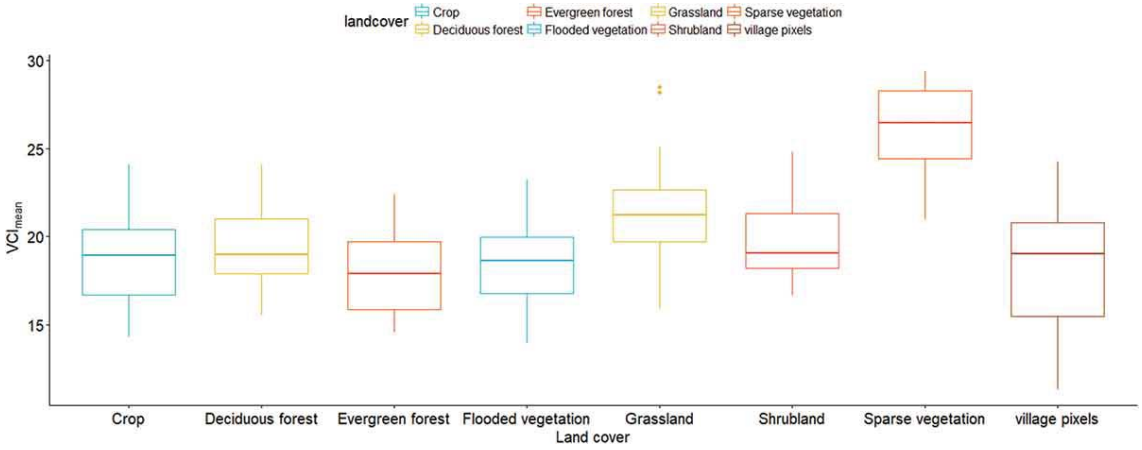

Figure 4. Box-plots showing the comparison of drought impacts (VCI_{mean}) among land cover types.

The mean VCI values for the land cover types are presented in Table 3. The lowest mean VCI values were recorded in the evergreen forest (VCI = 17.89) and the flooded vegetation (VCI = 18.05). On the other end, the highest VCI value of 26.04 was recorded over the sparse vegetation.

Table 3. Mean VCI per land cover.

Land cover	VCI_{mean}
Crop	18.77
Deciduous forest	19.36
Evergreen forest	17.89
Flooded vegetation	18.05
Grassland	21.47
Shrubland	19.80
Sparse vegetation	26.04
Village pixels	18.31

3.2. Vegetation response to drought per land cover type

Table 4 presents a summary of the response of each land cover type to drought impact. Our findings show that most land cover types generally responds to drought impacts at time scales ranging from 2 months to 8 months. Cropland and respond to drought at short time scales (i.e. 2 months) whereas flooded vegetation responds at medium time scales (i.e. 8 months). These results are consistent with the findings of (Vicente-Serrano 2007).

Table 4. SPEI times-scale with the highest correlation between NDVI and SPEI (time-lag of drought impact on land cover).

Land cover	Time-lag of drought impact (months)
Crop	2
Evergreen forest	3
Deciduous forest	4
Shrubland	5
Grassland	6
Sparse vegetation	7
Flooded vegetation	8

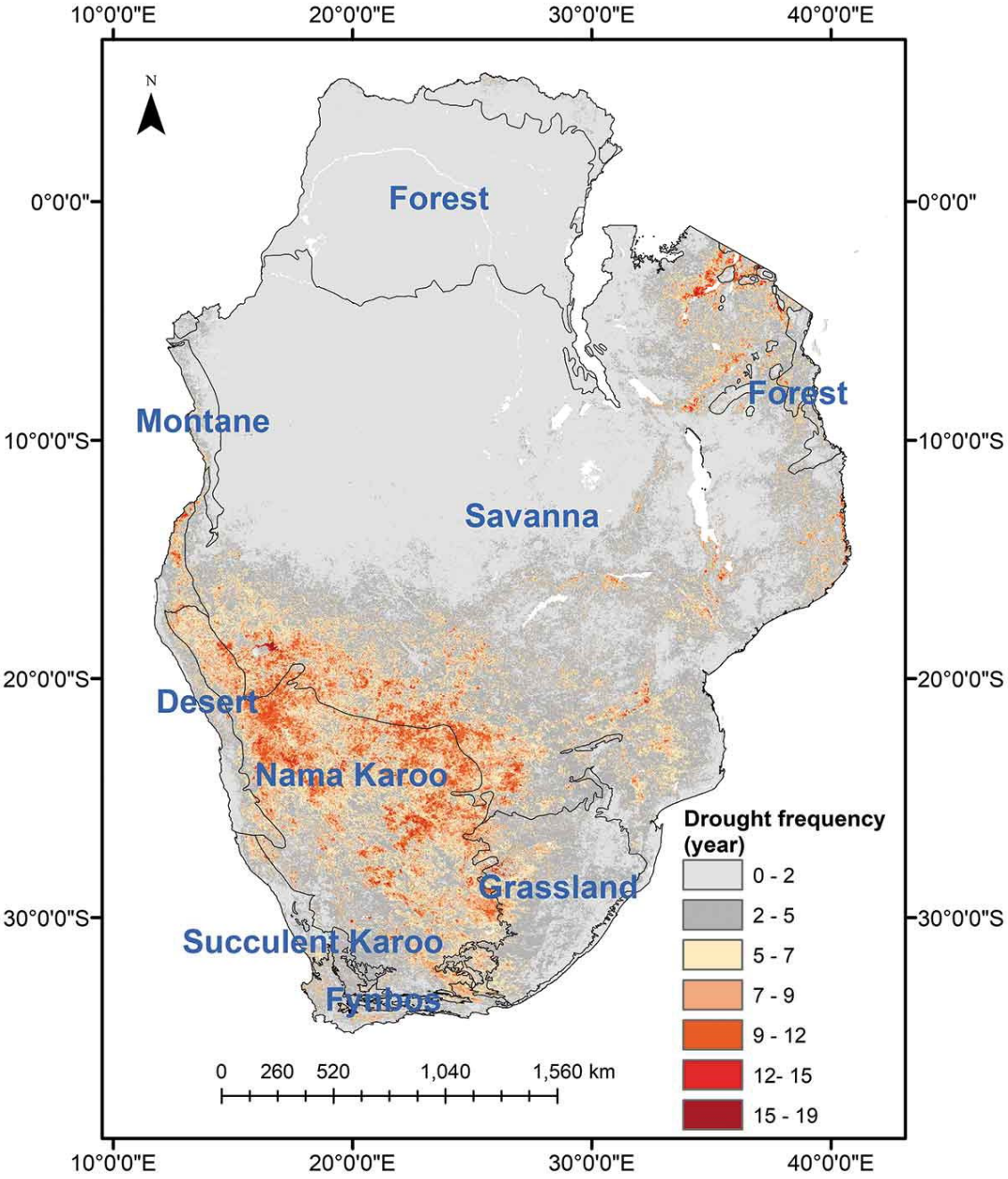

Figure 5. Drought frequency map (1998–2018).

3.3. Drought impact frequency map

Figure 5 shows the drought frequency (i.e. the number of years each pixel experienced drought conditions) between 1998 to 2018. Results of the drought impact frequency analysis show that the highest drought frequency is found in the south western parts of the study area mainly covering the grasslands and crops land cover which generally lies within the Karoo and southern parts of the savanna biomes (Figure 5). On the other hand, the northern half of the study area has the least drought frequency. The low drought frequency over the desert is due to the fact that most parts of the desert contain bare areas which were masked out together with waterbodies and irrigated cropped areas.

4. Discussion and conclusion

In this study, we analysed the drought and land cover interaction by comparing the 2015 to 2016 drought impact on different vegetation cover types using VCI. We also developed a novel land cover map, the 'village pixels' based on livestock density. The village pixel land cover provides a proxy for rural communities. The inclusion of the 'village pixels' or 'social pixel' is novel and important since it provides a new insight into drought impacts on rural communities. To the best of our knowledge, no study has specifically focused on drought impact on rural communities based on the village pixel approach. This helps to identify and prioritize drought relief to the village communities at risk during a drought event. Furthermore, the response of each land cover to drought impact was calculated by correlating the NDVI and SPEI.

Our results show that drought impacts on vegetation vary with land use and land cover type. The sparse vegetation appears to be the least affected by the 2015 to 2016 drought. This can be explained by the fact that this land cover together with the grassland quickly responds to rainfall after the termination of drought which leads to vegetation greening up (Vicente-Serrano 2007). On the other hand, the evergreen forest and the flooded vegetation recorded the lowest VCI (highest drought impact). The low VCI for the Flooded vegetation might be explained by the fact that greater parts of the vegetation Flooded cover lie in the arid part of the region (e.g. the Okavango delta) which means more drought impacts during drought period. For the evergreen forest, the low VCI could be explained by the fact that the forest quickly responds to drought impact (Table 4). Deciduous forests on the other hand are less impacted by drought (VCI = 19.36) compared to evergreen forest (VCI = 17.89). This can due to the fact that, unlike the evergreen forests, deciduous trees normally shed leaves as a copying strategy to minimize drought impacts (Chidumayo 2001)

Despite the fact that the 'village pixel' land cover class had a mean VCI of 18.31, much higher than the evergreen forest vegetation, it is worrying to note that the lowest dekadal VCI values were located in the 'village pixels' (Figure 4). It is reasonable to hypothesize that the 'village pixel' land cover type is vulnerable to drought impact due to browsing and clearing of land for settlements. This finding is worrying considering the important role of the 'village pixels' in supporting rural communities. In terms of the drought frequency, the highest frequency was found mainly in the southwestern parts of the region mostly covering the grassland and crop land cover type. On the other hand, the forest land cover had the least drought frequency. The low VCI values recorded across the land cover types are in line

with the finding of Archer et al. (2017) who also analysed the 2015 to 2016 season and reported widespread drought across many countries in Southern Africa.

By analysing the drought and land cover interactions, the response of the land cover to the drought impact and drought impact frequency, we were able to characterize both the spatio-temporal analysis of drought impact across different land cover classes. The results of this study provide information that can be used to support land use planning e.g. land-use zoning which is informed by the sensitivity of the land cover to drought impact. The results also provide baseline information for setting up of drought early warning systems which are based on the time lag of vegetation response to drought. To improve the results especially of the vegetation response to drought impact (i.e. correlation of the SPEI and NDVI) we recommend that future studies consider finer temporal resolution of the SPEI dataset. This study was limited by the temporal resolution of the SPEI data which is freely available at 1-month temporal resolution which can affect the correlation results.

Disclosure statement

The authors declare no conflict of interest.

Author contribution

Study conception and design: Marumbwa, Cho

Acquisition of data: Marumbwa

Analysis and interpretation of data: Marumbwa, Cho

Drafting of manuscript: Marumbwa

Supervision: Cho and Chirwa

Critical revision: Cho, Marumbwa

Funding

This work was supported by the University of Pretoria Postgraduate Doctoral Bursary.

References

Archer, E., R. Mary, W. A. Landman, M. A. Tadross, J. Malherbe, H. Weepener, P. Maluleke, and F. M. Marumbwa . 2017. "Understanding the Evolution of the 2014–2016 Summer Rainfall Seasons in Southern Africa: Key Lessons." *Climate Risk Management* 16: 22–28. doi: 10.1016/j.crm.2017.03.006.

Ayanlade, A., M. Radeny, J. F. Morton, and T. Muchaba. 2018. "Rainfall Variability and Drought Characteristics in Two Agro-climatic Zones: An Assessment of Climate Change Challenges in Africa." *Science of the Total Environment* 630: 728–737. doi: 10.1016/j.scitotenv.2018.02.196.

Baniya, B., Q. Tang, X. Ximeng, G. G. Haile, and G. Chhipi-Shrestha. 2019. "Spatial and Temporal Variation of Drought Based on Satellite Derived Vegetation Condition Index in Nepal from 1982–2015." *Sensors (Basel, Switzerland)* 19 (2): 430. doi:10.3390/s19020430.

Beguería, S., S. M. Vicente-Serrano, F. Reig, and B. Latorre. 2014. "Standardized Precipitation Evapotranspiration Index (SPEI) Revisited: Parameter Fitting, Evapotranspiration Models, Tools, Datasets and Drought Monitoring." 34 (10): 3001–3023. doi:10.1002/joc.3887.

Chidumayo, E. N. 2001. "Climate and Phenology of Savanna Vegetation in Southern Africa." *Journal of Vegetation Science* 12 (3): 347–354. doi:10.2307/3236848.

Cho, M. A., A. Ramoelo, and L. Dziba. 2017. "Response of Land Surface Phenology to Variation in Tree Cover during Green-Up and Senescence Periods in the Semi-Arid Savanna of Southern Africa." 9 (7): 689. doi:10.3390/rs9070689.

Cousins, B. 1999. "Invisible Capital: The Contribution of Communal Rangelands to Rural Livelihoods in South Africa." *Development Southern Africa* 16 (2): 299–318. doi:10.1080/03768359908440079.

Dai, A. 2013. "Increasing Drought under Global Warming in Observations and Models." *Nature Climate Change* 3 (1): 52. doi:10.1038/nclimate1633.

Davis-Reddy, C. L., and K. Vincent. 2017. *Climate Risk and Vulnerability: A Handbook for Southern Africa*. 2nd ed. Pretoria, South Africa: CSIR.

Dutta, D., A. Kundu, N. R. Patel, S. K. Saha, and A. R. Siddiqui. 2015. "Assessment of Agricultural Drought in Rajasthan (India) Using Remote Sensing Derived Vegetation Condition Index (VCI) and Standardized Precipitation Index (SPI)." *The Egyptian Journal of Remote Sensing and Space Science* 18 (1): 53–63. doi: 10.1016/j.ejrs.2015.03.006.

Ellis-Jones, J., and D. O'Neill. 2000. "The Contribution of Draught Animal Power to Sustainable Livelihoods in Sub-Saharan Africa: An Example from Zimbabwe." In *World Association for Transport Animal Welfare and Studies (TAWS) Workshop Harare,*

Zimbabwe. ESA . 2019. “GlobCover.” Accessed November 11 http://due.esrin.esa.int/page_globcover.php

Gidey, E., O. Dikinya, R. Sebego, E. Segosebe, and A. Zenebe. 2018. “Analysis of the Long-term Agricultural Drought Onset, Cessation, Duration, Frequency, Severity and Spatial Extent Using Vegetation Health Index (VHI) in Raya and Its Environs, Northern Ethiopia.” *Environmental Systems Research* 7 (1): 13. doi:10.1186/s40068-018-0115-z.

Gouveia, C. M., R. M. Trigo, S. Beguería, and S. M. Vicente-Serrano. 2017. “Drought Impacts on Vegetation Activity in the Mediterranean Region: An Assessment Using Remote Sensing Data and Multi-scale Drought Indicators.” *Global and Planetary Change* 151: 15–27. doi: 10.1016/j.gloplacha.2016.06.011.

Jain, S. K., R. Keshri, A. Goswami, A. Sarkar, and A. Chaudhry. 2009. “Identification of Drought-vulnerable Areas Using NOAA AVHRR Data.” *International Journal of Remote Sensing* 30 (10): 2653–2668. doi:10.1080/01431160802555788.

Kogan, F., W. Guo, and W. Yang. 2019. “Drought and Food Security Prediction from NOAA New Generation of Operational Satellites.” *Geomatics, Natural Hazards and Risk* 10 (1): 651–666. doi:10.1080/19475705.2018.1541257.

Kogan, F. N. 1990. “Remote Sensing of Weather Impacts on Vegetation in Non-homogeneous Areas.” *International Journal of Remote Sensing* 11 (8): 1405–1419. doi:10.1080/01431169008955102.

Kogan, F. N. 1995. “Application of Vegetation Index and Brightness Temperature for Drought Detection.” *Advances in Space Research* 15 (11): 91–100. doi:10.1016/0273-1177(95)00079-T.

Kogan, F. N. 1997. “Global Drought Watch from Space.” *Bulletin of the American Meteorological Society* 78 (4): 621–636. doi:10.1175/1520-0477(1997)078<0621:GDWFS>2.0.CO;2.

Kruskal, W. H., and W. A. Wallis. 1952. “Use of Ranks in One-criterion Variance Analysis.” *Journal of the American Statistical Association* 47 (260): 583–621. doi:10.1080/01621459.1952.10483441.

Kuri, F., M. Masocha, A. Murwira, and K. Murwira. 2019. “Differential Impact of Remotely Sensed Dry Dekads on Maize Yield in Zimbabwe.” *Geocarto International* 1–11. doi:10.1080/10106049.2019.1583774.

Lindesay, J. A. 1988. “South African Rainfall, the Southern Oscillation and a Southern Hemisphere Semi-annual Cycle.” 8 (1): 17–30. doi:10.1002/joc.3370080103.

Liu, W. T., and F. N. Kogan. 1996. “Monitoring Regional Drought Using the Vegetation Condition Index.” *International Journal of Remote Sensing* 17 (14): 2761–2782. doi:10.1080/01431169608949106.

Nicholson, S. E., M. L. Davenport, and A. R. Malo. 1990. “A Comparison of the Vegetation Response to Rainfall in the Sahel and East Africa, Using Normalized Difference Vegetation Index from NOAA-AVHRR.” *Climate Change* 17: 209–241. doi:10.1007/BF00138369.

Pearson, R. A., and E. Vall. 1998. “Performance and Management of Draught Animals in Agriculture in sub-Saharan Africa: A Review.” *Tropical Animal Health and Production* 30 (5): 309–324. doi:10.1023/a:1005059308088.

R Core Team. 2018. *R: A Language and Environment for Statistical Computing* . Vienna, Austria: R Foundation for Statistical Computing.

Robinson, T. P., G. R. W. Wint, G. Conchedda, T. P. Van Boeckel, V. Ercoli, E. Palamara, G. Cinardi, L. D’Aietti, S. I. Hay, and M. Gilbert. 2014. “Mapping the Global Distribution of Livestock.” *PloS One* 9 (5): 5. doi: 10.1371/journal.pone.0096084.

Rojas, O., and S. Ahmed. 2017. “Feasibility of Using the FAO-Agricultural Stress Index System (ASIS) as a Remote Sensing Based Index for Crop Insurance.” Accessed May 29 2017. http://repo.floodalliance.net/jspui/handle/44111/1713

Swemmer, A. M., W. J. Bond, G. P. Jason Donaldson, J. M. Hempson, and P. J. S. Izak. 2018. “The Ecology of Drought – A Workshop Report.” *South African Journal of Science* 114 (9/10): 1–3. doi:10.17159/sajs.2018/5098.

Tollerud, H., J. Brown, T. Loveland, R. Mahmood, and N. Bliss. 2018. “Drought and Land-Cover Conditions in the Great Plains.” 22 (17): 1–25. doi:10.1175/ei-d-17-0025.1.

Tucker, C. J., C. L. Vanpraet, E. Boerwinkel, and A. Gaston. 1983. “Satellite Remote Sensing of Total Dry Matter Production in the Senegalese Sahel.” *Remote Sensing of Environment* 13 (6): 461–474. doi:10.1016/0034-4257(83)90053-6.

Unganai, L. S., and F. N. Kogan. 1998. “Drought Monitoring and Corn Yield Estimation in Southern Africa from AVHRR Data.” *Remote Sensing of Environment* 63 (3): 219–232. doi:10.1016/S0034-4257(97)00132-6.

UN-SPIDER. 2019. “Recommended Practice: Drought Monitoring Using the Vegetation Condition Index (VCI).” Accessed 10 January 2019. http://www.un-spider.org/book/export/html/9206

Van Loon, A. F. 2015. “Hydrological Drought Explained.” 2 (4): 359–392. doi:10.1002/wat2.1085.

Vargha, A., and H. D. Delaney. 1998. “The Kruskal-Wallis Test and Stochastic Homogeneity.” *Journal of Educational and Behavioral Statistics* 23 (2): 170–192. doi:10.3102/10769986023002170.

Vicente-Serrano, S. 2007. “Evaluating the Impact of Drought Using Remote Sensing in a Mediterranean, Semi-arid Region.” *Natural Hazards* 40 (1): 173–208. doi:10.1007/s11069-006-0009-7.

Vicente-Serrano, S. M., C. Gouveia, J. J. Camarero, S. Beguería, R. Trigo, J. I. López-Moreno, C. Azorín-Molina, et al. 2013. “Response of Vegetation to Drought Time-scales across Global Land Biomes.” *Proceedings of the National Academy of Sciences* 110 (1): 52–57. doi:10.1073/pnas.1207068110.

Vicente-Serrano, S. M., S. Beguería, and J. I. López-Moreno. 2010. “A Multiscalar Drought Index Sensitive to Global Warming: The Standardized Precipitation Evapotranspiration Index.” *Journal of Climate* 23 (7): 1696–1718. doi:10.1175/2009JCLI2909.1.

Wilhite, D. A. 2000. “Drought as A Natural Hazard: Concepts and Definitions. In Drought: A Global Assessment.” *Drought Mitigation Center Faculty Publications* 1: 3–18.

Wolters, E., E. Swinnen, C. Tote, and S. Sterclkx. 2016. *SPOT-VGT Collection 3 Products and User Manual*.

Zaiontz, C. 2019. “Real Statistics Using Excel: Kruskal-Wallis Test.” Accessed 11 November 2019. http://www.real-statistics.com/one-way-analysis-of-variance-anova/kruskal-wallis-test/